

# Tackling the Curse of Data Imbalancing for Melanoma Classification

Mojdeh Rastgoo, Guillaume Lemaître, Rafael Garcia  
Universitat de Girona  
Campus Montilivi, Edifici P4, 17071 Girona

Joan Massich, Olivier Morel, Fabrice Mériaudeau, Franck Marzani  
Université de Bourgogne Franche-Comté  
12 rue de la Fonderie, 71200 Le Creusot

## Abstract

*Malignant melanoma is the most dangerous type of skin cancer, yet melanoma is the most treatable kind of cancer when diagnosed at an early stage. In this regard, Computer-Aided Diagnosis systems based on machine learning have been developed to discern melanoma lesions from benign and dysplastic nevi in dermoscopic images. Similar to a large range of real world applications encountered in machine learning, melanoma classification faces the challenge of imbalanced data. This article is devoted to analyze the impact of data balancing strategies at the training step. Subsequently, an extensive comparison between Over-Sampling (OS) and Under-Sampling (US), in both feature and data space is performed revealing the fact that NearMiss-2 (NM2) outperforms other methods achieving Sensitivity (SE) and Specificity (SP) of 92.50% and 77.50%, respectively. More generally, the reported results highlight that methods based on OS in data space and US in feature space outperform the others.*

## 1. Introduction

Malignant melanoma is the deadliest type of skin cancer, accounting for the vast majority of skin cancer deaths [1]. According to latest reports, melanoma causes over 20,000 deaths annually in Europe [2]. In 2014, the American Cancer Society also reported that the number of new diagnosed cases is 76,100 with 9710 estimated deaths [1]. Nevertheless, melanoma is the most treatable kind of cancer if diagnosed early.

The clinical diagnosis of early stage melanoma is commonly based on the “ABCDE” rule [3], defined as Asymmetry, irregular Borders, variegated Colours, Diameters greater than 6 mm and Evolving stages over time. In addition, the clinical diagnosis of melanoma is performed through visual inspection and deep analysis of the lesion,

using clinical imaging techniques such as dermoscopic imaging. However, these inspections and analysis are not easy tasks due to challenges such as similarity of the different lesion types (dysplastic and melanoma) and the necessity to perform patient follow-up over years. Therefore, the research communities have dedicated their efforts to develop computerized lesion analysis algorithms for classification of melanoma lesions. However, akin to other medical applications, the percentage of melanoma cases in comparison with benign and dysplastic cases is far less. This problem is frequently referred as “class imbalanced” problem [4] and has been encountered in multiple areas such as telecommunication managements, bioinformatics, fraud detection, and medical diagnosis. Imbalanced data substantially compromise the learning process since most of the standard machine learning algorithms expect balanced class distribution or an equal misclassification cost [5].

Medical data are prone to such drawbacks due to the fact that the portion of diseased samples or patients is far lower than healthy cases. Furthermore, the detection and classification of minority malignant cases are highly essential so that the Sensitivity (SE) of developed algorithms needs to be maximized. Consequently, the problem of imbalanced data is usually addressed by employing different techniques which do not vitiate the topology of the data. Despite the fact that classification of malignant melanoma has been extensively studied [6], up to our knowledge, only two works tackled the issue implied by imbalanced dataset [7], [8]. Barata *et al.* generate new synthetic samples by adding a Gaussian noise with fixed parameters to the samples belonging to the minority class [7]. Celebi *et al.* over-sampled their dataset using Synthetic Minority Over-sampling TEchnique (SMOTE) [9] to improve the SE of their algorithm [8].

This paper provides an insight to the specific problem of classification of imbalanced dataset for melanoma. To proceed, we review different techniques proposed by the

machine learning community and compile a comprehensive quantitative evaluation. The rest of this paper is organized as follows: an overview of the classification framework designed to investigate data balancing techniques is presented in Sect. 2 while these strategies are described in Sect. 3. A quantitative evaluation is discussed in Sect. 4 followed by a concluding section.

## 2. Material and Methods

Figure 1 illustrates and summarizes the experiment designed to explore the data imbalance problem during the classification of dermoscopic images. The experimentation is based on the works presented in [6], [10] and follows a cross-validated classification evaluation framework. Details of the dataset used for the experiments are given in Sect. 2.1. The extracted features correspond to the highest performing subset of features according to the latter mentioned studies and are summarized in Sect. 2.2. The classification is performed using a Random Forests (RF) classifier with 100 unpruned trees using gini criterion. The validation model used is a 10-fold cross-validation in which 80 % of the data are used for training and 20 % are used for testing. Furthermore, we dedicate an entire section (see Sect. 3) to focus on the different balancing strategies.

### 2.1. Dataset

The  $PH^2$  dermoscopic dataset which is acquired at *Dermatology Service of Hospital Pedro Hispano, Matosinhos, Portugal* is used [7]. The dermoscopic dataset is acquired with Tuebinger Mole Analyzer system with a magnification of  $20\times$ . The 8-bits RGB color dermoscopic images were obtained under the same conditions with a resolution of  $768\text{ px} \times 560\text{ px}$ . This dataset contains 200 dermoscopic images divided into 160 benign and dysplastic and 40 melanoma lesions. Moreover, each lesion is segmented and histological diagnosis are provided. In this study, we conducted the experiments with a subset of 39 melanoma and 117 benign and dysplastic lesions with an imbalance ratio of 1:3.

### 2.2. Feature extraction

**Color variance and histogram ( $C_1$ )** descriptors contain the mean and variance of the nine channels (R, G, B, H, S, V, L, A, B) and the histogram of the R, G and B channels.

**Opponent color space angle and Hue histogram ( $C_2$ )** is a robust and rotation invariant feature descriptor

derived from the RGB channels [11]:

$$\begin{aligned} H &= \arctan \left( \frac{\sqrt{3}(R - G)}{R + G - 2B} \right), \\ \theta_d^O &= \arctan \left( \frac{\sqrt{3}(R'_d - G'_d)}{R'_d + G'_d - 2B'_d} \right), \end{aligned} \quad (1)$$

where  $d$  denotes the spatial coordinates of  $(x, y)$  and  $R'_d, G'_d, B'_d$  denote the first order derivatives of RGB channels with respect to the coordinates. The color descriptor is built by taking histogram of the opponent angle  $\theta_d^O$  and the hue channel ( $H$ ).

**Completed Local Binary Pattern (CLBP) ( $T_1$ )** is a completed modeling of Local Binary Pattern, especially designed for texture classification [12]. This descriptor encodes the magnitude and sign differences of the central pixel with its neighbors in the local patterns rather than only the sign differences. The CLBP are calculated for each pixel in a given image and their histogram defines the final descriptor.

**Gabor filter ( $T_2$ )** is a linear filter which is defined as a modulation of a Gaussian kernel with a sinusoidal wave. This filter is formulated in Eq. (2) as two Gaussian with standard deviations of  $\sigma_x$  and  $\sigma_y$  that vary along  $x$  and  $y$  axes and it is modulated by a complex sinusoidal with a wavelength of  $\lambda$ . Here  $\theta$  represents the orientation of the Gabor filter,  $\psi$  is the phase offset and  $s$  is the scale factor. The filter bank is created using six different orientations equally spaced in the interval  $[0, \pi]$ , along 4 scales with a downsizing factor of 2:

$$g(x, y) = \exp \left( - \left( \frac{x'^2}{2\sigma_x^2} + \frac{y'^2}{2\sigma_y^2} \right) \right) \cos \left( 2\pi \frac{x'}{\lambda} + \psi \right), \quad (2)$$

where

$$\begin{aligned} x' &= s(x \cos \theta + y \sin \theta), \\ y' &= s(-x \sin \theta + y \cos \theta). \end{aligned}$$

## 3. Balancing strategies

Considering a binary classification problem, the class with the smallest number of samples is defined as the *minority* class and its counterpart is defined as the *majority* class. The problem of data balancing corresponds to equalizing the number of samples of both the minority and majority classes. This task can be achieved in either data or feature space.

### 3.1. Data space sampling

Data space sampling is related with the generation of new synthetic samples by modifying the original data ahead

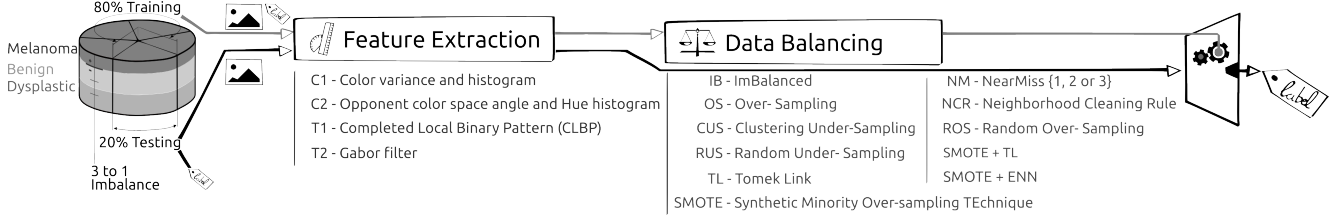


Figure 1: Framework outline

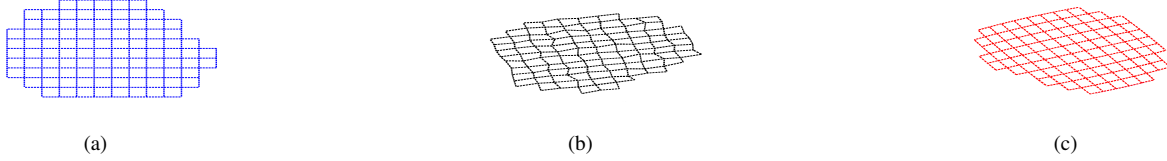


Figure 2: Data space transformation: (a) original synthetic data, (b) RDGM deformation, (c) BD deformation.

of any feature extraction processes. Over-Sampling (OS) is performed on the original dataset by generating synthetic melanoma images based on two types of deformation [10]. Furthermore, cubic b-spline interpolation is used with both methods to approximate non-integer points in the image.

**Random Deformation using Gaussian Motion** achieved by deforming the original image by adding a random Gaussian motion  $\mathcal{N}(\mu, \sigma) = (5, 5)$  at each pixel compounded with a global rotation of  $80^\circ$ .

**Barrel Deformation** corresponds to a deformation of the original image using barrel distortion compounded with a global rotation of  $145^\circ$ .

A synthetic example illustrating the results of these deformation is presented in Fig. 2.

### 3.2. Feature space sampling

Considering the problem of imbalanced, Under-Sampling (US) is performed such that the number of samples of the majority class is reduced to be equal to the number of samples of the minority class. The following methods are considered to perform such balancing.

**Random Under-Sampling** is performed by randomly selecting without replacement a subset of samples from the majority class such that the number of samples is then equal in both minority and majority classes.

**Tomek Link (TL)** can be used to under-sample the majority class of the original dataset [13]. Let define a pair of Nearest Neighbour (NN) samples  $(x_i, x_j)$  such that their associated class label  $y_i \neq y_j$ . The pair  $(x_i, x_j)$

is defined as a TL if, by relaxing the class label differentiation constraint, there is no other sample  $x_k$  defined as the NN of either  $x_i$  or  $x_j$ . US is performed by removing the samples belonging to the majority class and forming a TL. It can be noted that this US strategy does not enforce a strict balancing between the majority and the minority classes.

**Clustering Under-Sampling** refers to the use of a  $k$ -means to cluster the feature space such that  $k$  is set to be equal to the number of samples composing the minority class. Hence, the centroids of the OASE clusters define the new samples of the majority class.

**NearMiss (NM)** offers three different methods to under-sample the majority class [14]. In NearMiss-1 (NM1), samples from the majority class are selected such that for each sample, the average distance to the  $k$  NN samples from the minority class is minimum. NearMiss-2 (NM2) diverges from NM1 by considering the  $k$  farthest neighbours samples from the minority class. In NearMiss-3, a subset  $M$  containing samples from the majority class is generated by finding the  $m$  NN from each sample of the minority class. Then, samples from the subset  $M$  are selected such that for each sample, the average distance to the  $k$  NN samples from the minority class is maximum. In our experiment,  $k$  and  $m$  are fixed to 3.

**Neighborhood Cleaning Rule (NCR)** consists of applying two rules depending on the class of each sample [15]. Let define  $x_i$  as a sample of the dataset with its associated class label  $y_i$ . Let define  $y_m$  as the class of the majority vote of the  $k$  NN of the sample  $x_i$ . If  $y_i$  corresponds to the majority class and  $y_i \neq y_m$ ,  $x_i$

Table 1: The obtained results with different balancing techniques for color and texture features using a RF classifier. The first and second highest results for each feature set are highlighted in dark and lighter gray colors, respectively.

Features	Color						Texture						Combined					
	$C_1$		$C_2$		$C_{1,2}$		$T_1$		$T_2$		$T_{1,2}$		$T_1, C_{1,2}$		$T_2, C_{1,2}$		$T_{1,2}, C_{1,2}$	
Balancing techniques	SE	SP	SE	SP	SE	SP	SE	SP	SE	SP	SE	SP	SE	SP	SE	SP	SE	SP
IB	52.50	89.58	75.00	88.75	71.25	87.50	38.75	91.67	60.00	96.25	66.25	93.75	73.75	89.58	71.25	89.58	71.25	92.50
OS	93.75	66.67	80.00	86.25	82.50	87.08	43.75	83.75	72.50	90.00	70.00	91.67	77.50	87.08	81.25	88.33	78.75	88.33
ROS	55.00	80.83	80.00	84.17	72.50	85.42	42.50	82.08	60.00	89.17	66.25	87.92	75.00	85.42	73.75	86.25	73.75	85.83
SMOTE	60.00	82.50	78.75	84.58	75.00	70.00	56.25	74.17	61.25	87.50	84.17	87.08	78.75	85.00	73.75	84.58	73.75	85.00
RUS	72.50	72.92	86.25	80.00	78.75	80.00	67.50	53.33	76.25	76.25	85.00	78.75	91.25	75.00	85.00	78.75	92.50	78.33
TL	51.25	86.25	76.25	87.92	67.50	88.33	37.50	87.92	65.00	90.42	68.75	91.67	73.75	88.75	63.75	90.00	72.50	91.25
CUS	81.25	67.92	80.00	84.58	86.25	80.42	56.25	65.83	70.00	77.50	85.00	77.08	83.75	81.25	80.00	84.17	83.75	82.92
NM1	67.50	72.08	86.25	79.17	85.00	82.50	72.50	43.75	80.00	62.50	87.50	66.67	85.00	82.08	86.25	80.42	87.50	80.83
NM2	70.00	72.92	86.25	81.25	85.00	82.92	76.25	48.75	86.25	40.83	86.25	51.25	87.50	82.08	92.50	77.50	91.25	81.67
NM3	82.50	75.00	87.50	80.83	85.00	80.42	73.75	55.83	72.50	82.50	82.50	80.42	83.75	81.25	85.00	80.00	86.25	80.42
NCR	66.25	76.67	87.50	81.25	85.00	82.08	67.50	67.92	75.00	85.83	82.50	83.33	86.25	81.67	82.50	85.00	83.75	85.42
SMOTE + ENN	76.25	73.33	85.00	81.25	85.00	82.08	81.25	56.25	76.25	82.08	80.00	79.58	86.25	81.25	83.75	82.50	78.75	82.92
SMOTE + TL	75.00	73.75	83.75	82.50	87.50	80.83	72.50	59.17	77.50	82.08	78.75	78.75	85.00	82.08	77.50	82.92	88.75	82.50

is rejected from the final subset. If  $y_i$  corresponds to the minority class and  $y_i \neq y_m$ , then the  $k$  NN are rejected from the final subset.

In the contrary, the data balancing can be performed by OS in which the new samples belonging to the minority class are generated aiming at equalizing the number of samples in both classes. Two different methods are considered.

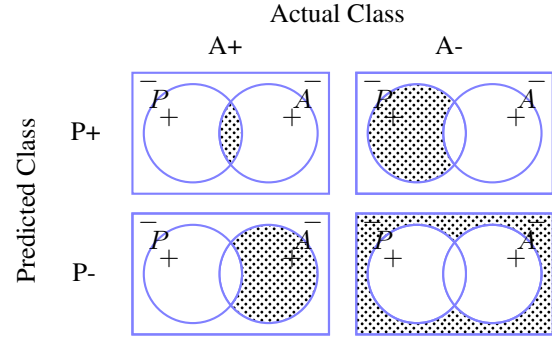
**Random Over-Sampling** is performed by randomly replicating the samples of the minority class such that the number of samples is equal in both minority and majority classes.

**SMOTE** is a method to generate synthetic samples in the feature space [9]. Let define  $x_i$  as a sample belonging to the minority class. Let define  $x_{nn}$  as a randomly selected sample from the  $k$  NN of  $x_i$ . Therefore, a new sample  $x_j$  is generated such that  $x_j = x_i + \sigma(x_{nn} - x_i)$ , where  $\sigma$  is a random number in the interval  $[0, 1]$ .

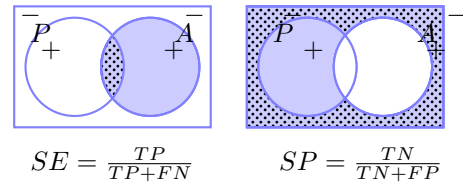
Subsequently, OS methods can be combined with US methods to clean the subset created. In that regard, two different combinations are tested.

**SMOTE + TL** are combined to clean the samples created using SMOTE [16]. SMOTE over-sampling can lead to overfitting which can be avoided by removing the TL from both majority and minority classes [4].

**SMOTE + Edited Nearest Neighbour** are combined for the same aforementioned reason [17].



(a) Confusion matrix with truly and falsely positive samples detected (TP, FP) in the first row, from left to right and the falsely and truly negative samples detected (FN, TN) in the second row, from left to right.



(b) Sensitivity and Specificity evaluation, corresponding to the ratio of the dotted area over the blue area.

Figure 3: Evaluation metrics: (a) confusion matrix, (b) Sensitivity - Specificity

## 4. Experimental Results

The classification results are reported in Table 1 using the aforementioned features, the RF classifier and the different imbalancing techniques presented in Sect. 3. These results are compiled in terms of average SE and Specificity (SP) over 10 runs of the cross-validation. The visual and

analytic interpretation of these evaluation measures are depicted in Fig. 3. Table 1 can be divided into three main parts representing the results using imbalance data (IB), the balancing in the data space OS and the balancing in the feature space. These strategies are separated by a double horizontal line. The strategies performed in the feature space are subdivided into either OS or US or a combination of OS follow by US (see horizontal dashed line in Table 1). The two highest SE for each feature set are highlighted in dark and light gray cell colors, respectively.

The obtained results indicate that balancing techniques are essential and improve the classification performance. However, the improvements in comparison to imbalanced classification is evident. For this case study the US techniques outperform the OS techniques. Due to the characteristics similarities of melanoma and dysplastic lesions, it is expected to have correlated feature space among melanoma and dysplastic lesions. Subsequently, the miss-leading samples could be removed using US and lead to better performance. Specifically to our purpose, NM2 is the algorithm maximizing the sensitivity and in overall, NM algorithms perform the best on our dataset. However, NCR algorithm (see results highlighted in blue in Table 1) achieves the best performance, considering a trade-off between SE and SP. Focusing only on OS techniques, OS in data space outperforms the techniques performing in feature space.

## 5. Conclusion

In this paper, we analyzed the impact of data balancing techniques for the classification of malignant melanoma. Therefore, we presented an extensive comparison of twelve OS and US techniques in both feature and data space. These techniques were evaluated on a subset of  $PH^2$  dataset with an imbalanced ration of 1:3. The obtained results particularly highlight the advantage of balancing the training set over using the original data, particularly for the methods based on OS in data space and US in feature space (NM).

## References

- [1] A. C. Society, *Cancer facts & figures 2014*, 2014. [Online]. Available: <http://www.cancer.org/research/cancerfactsstatistics/cancerfactsfigures2014> (cit. on p. 1).
- [2] A. Forsea, V. Del Marmol, E. de Vries, E. Bailey, and A. Geller, "Melanoma incidence and mortality in europe: new estimates, persistent disparities," *British Journal of Dermatology*, vol. 167, no. 5, pp. 1124–1130, 2012 (cit. on p. 1).
- [3] N. R. Abbasi, H. M. Shaw, *et al.*, "Early diagnosis of cutaneous melanoma: revisiting the abcd criteria," *Jama*, vol. 292, no. 22, pp. 2771–2776, 2004 (cit. on p. 1).
- [4] R. C. Prati, G. E. Batista, and M. C. Monard, "Data mining with imbalanced class distributions: concepts and methods.," in *IICAI*, 2009, pp. 359–376 (cit. on pp. 1, 4).
- [5] H. He, E. Garcia, *et al.*, "Learning from imbalanced data," *Knowledge and Data Engineering, IEEE Transactions on*, vol. 21, no. 9, pp. 1263–1284, 2009 (cit. on p. 1).
- [6] M. Rastgoo, R. Garcia, O. Morel, and F. Marzani, "Automatic differentiation of melanoma from dysplastic nevi," *Computerized Medical Imaging and Graphics*, vol. 43, pp. 44–52, 2015 (cit. on pp. 1, 2).
- [7] C. Barata, M. Ruela, M. Francisco, T. Mendonça, and J. Marques, "Two systems for the detection of melanomas in dermoscopy images using texture and color features," *IEEE Systems Journal*, vol. 8, no. 3, pp. 965–979, Sep. 2014 (cit. on pp. 1, 2).
- [8] M. E. Celebi, H. A. Kingravi, *et al.*, "A methodological approach to the classification of dermoscopy images," *Computerized Medical Imaging and Graphics*, vol. 31, no. 6, pp. 362–373, 2007 (cit. on p. 1).
- [9] N. V. Chawla, K. W. Bowyer, L. O. Hall, and W. P. Kegelmeyer, "Smote: synthetic minority over-sampling technique," *Journal of artificial intelligence research*, pp. 321–357, 2002 (cit. on pp. 1, 4).
- [10] M. Rastgoo, O. Morel, F. Marzani, and R. Garcia, "Ensemble approach for differentiation of malignant melanoma," in *The International Conference on Quality Control by Artificial Vision 2015*, International Society for Optics and Photonics, 2015, pp. 953 415–953 415 (cit. on pp. 2, 3).
- [11] J. Van De Weijer and C. Schmid, "Coloring local feature extraction," in *Computer Vision—ECCV 2006*, Springer, 2006, pp. 334–348 (cit. on p. 2).
- [12] Z. Guo and D. Zhang, "A completed modeling of local binary pattern operator for texture classification," *IEEE Transactions on Image Processing*, vol. 19, no. 6, pp. 1657–1663, 2010 (cit. on p. 2).
- [13] I. Tomek, "Two modifications of cnn," *IEEE Trans. Syst. Man Cybern.*, vol. 6, pp. 769–772, 1976 (cit. on p. 3).
- [14] I. Mani and I. Zhang, "Knn approach to unbalanced data distributions: a case study involving information extraction," in *Proceedings of Workshop on Learning from Imbalanced Datasets*, 2003 (cit. on p. 3).
- [15] J. Laurikkala, *Improving identification of difficult small classes by balancing class distribution*. Springer, 2001 (cit. on p. 3).

- [16] G. E. Batista, A. L. Bazzan, and M. C. Monard, “Balancing training data for automated annotation of keywords: a case study,” in *WOB*, 2003, pp. 10–18 (cit. on p. 4).
- [17] G. E. Batista, R. C. Prati, and M. C. Monard, “A study of the behavior of several methods for balancing machine learning training data,” *ACM Sigkdd Explorations Newsletter*, vol. 6, no. 1, pp. 20–29, 2004 (cit. on p. 4).